Assessment of optical path length in tissue using neodymium and water absorptions for application to near-infrared spectroscopy

Stephen P. Nighswander-Rempel
Valery V. Kupriyanov
R. Anthony Shaw
Institute for Biodiagnostics
435 Ellice Ave.
Winnipeg, Manitoba R3B 1Y6
E-mail: Anthony.Shaw@nrc-cnrc.gc.ca

Abstract. Quantitative analysis of blood oxygen saturation using near-IR spectroscopy is made difficult by uncertainties in both the absolute value and the wavelength dependence of the optical path length. We introduce a novel means of assessing the wavelength dependence of path length, exploiting the relative intensities of several absorptions exhibited by an exogenous contrast agent (neodymium). Combined with a previously described method that exploits endogenous water absorptions, the described technique estimates the absolute path length at several wavelengths throughout the visible/near-IR range of interest. Isolated rat hearts ($n=11$) are perfused separately with Krebs-Henseleit buffer (KHB) and a KHB solution to which neodymium had been added, and visible/near-IR spectra are acquired using an optical probe made up of emission and collection fibers in concentric rings of diameters 1 and 3 mm, respectively. Relative optical path lengths at 520, 580, 679, 740, 800, 870, and 975 nm are 0.41 ± 0.13, 0.49 ± 0.21, 0.90 ± 0.09, 0.94 ± 0.01, 1.00, 0.84 ± 0.01, and 0.78 ± 0.08, respectively. The absolute path length at 975 nm is estimated to be 3.8 ± 0.6 mm, based on the intensity of the water absorptions and the known tissue water concentration. These results are strictly valid only for the experimental geometry applied here.
 [DOI: 10.1117/1.1896372]

Keywords: neodymium; optical path length; visible; near-infrared; spectroscopy.

Paper 04060 received Apr. 14, 2004; revised manuscript received Sep. 24, 2004; accepted for publication Nov. 5, 2004; published online Apr. 26, 2005.

1 Introduction

Within the last twenty years near-IR spectroscopy (NIRS) has experienced a tremendous rise in use in a variety of biomedical applications. It has proven especially important in assessing blood oxygenation and hemoglobin (Hb) content.[1–3] However, accurate quantification of Hb levels *in vivo* has been hindered by the uncertainty in the optical path length. Spectroscopic measurements of chromophore concentrations make use of the Beer-Lambert law, which states that the absorbance is proportional to the molar absorptivity, the concentration, and the path length through the sample. In nonscattering media (such as *in vitro* solutions), the path length is simply the sample thickness, but in highly scattering media such as biological tissue, the effective path length can be many times the sample thickness or the interoptode spacing. If the path length is unknown, then only relative changes in concentration, rather than absolute values, can be derived from the measured spectra.

Scattering complicates the issue further in that the angular distribution of scattered light intensity is wavelength dependent. Since scattering (and absorption) is wavelength dependent, the path length is also wavelength dependent. Since absorbance is proportional to both concentration and path length, ignoring this wavelength dependence can lead to significant errors in spectroscopically derived chromophore concentrations, especially if only a few, discrete wavelengths are used in the analysis (as is the case in many marketed hemoximeters). Insights regarding the relative influences of scattering and absorption phenomena, and of probe geometry, have been gleaned from theoretical studies exploiting either Monte Carlo simulation of photon transport in tissue or using diffusion theory based on tissue optical constants.[4–6]

The technique that has been employed most often to estimate the absolute and relative path length in scattering media is time-resolved spectroscopy. Most studies utilizing this method, which measures the transit time for ultrashort laser pulses, have compared path lengths at two or three discrete wavelengths in the 690- to 860-nm near-IR range.[7–9] The usual gauge reported in these studies is the differential path length factor (DPF), defined as the mean path length (for a given wavelength) divided by the straight-line distance between the emitting and detecting optical fibers (optodes).

Relative and absolute DPF values from several relevant studies of skeletal muscle are compiled in Tables 1 and 2,

Address all correspondence to Dr. R. Anthony Shaw, National Research Council Canada, Institute for Biodiagnostics, 435 Ellice Avenue, Winnipeg, MB R3B 1Y6 Canada

1083-3668/2005/$22.00 © 2005 SPIE

Table 1 Summary of previous relative path length results.

Study	Relative Path Length Results
Klassen et al.[10]	DPF decreases with wavelength between 750 and 900 nm DPF (900 nm)=0.8×DPF (800 nm)
Pringle et al.[11]	No difference between DPF values at 744, 806, 834, and 860 nm
Kohl et al.[12]	DPF decreases with wavelength between 750 and 950 nm DPF (950 nm)=0.7×DPF (800 nm)
Duncan et al.[13]	DPF decreases with wavelength between 690 and 832 nm DPF (832 nm)=0.87×DPF (690 nm) in newborns
Benaron et al.[14]	No difference between DPF values at 754 and 816 nm
Duncan et al.[15]	DPF decreases with wavelength between 690 and 832 nm DPF (832 nm)=0.89×DPF (690 nm) in adults
Essenpreis et al.[9]	DPF decreases with wavelength between 740 and 840 nm DPF (840 nm)=0.9×DPF (740 nm)

respectively. These data indicate a slight decrease in DPF with increasing wavelength between 690 and 860 nm, and hence a corresponding decrease in optical path length.[9,11,15,17] However, the differences between the DPF values at the different wavelengths are small, and the intersubject variability in DPF values is high.[12,14] Moreover, DPF values are dependent on several factors other than the wavelength; these include tissue type, subject age, and source-detector separation and geometry. The reported DPF values range between 3 and 6 (indicating that the mean path length is several times the direct distance between probes), and the wide variation in absolute DPF values makes it difficult to determine absolute concentrations spectroscopically *in vivo* with any reliability.[13,18,19]

Table 2 Summary of previous absolute path length results.

Study	Absolute Path Length Results
Pringle et al.[11]	DPF (muscle)=5.4±1.0 (744 nm), 4.7±1.0 (860 nm), source-detector separation of 3 cm
Duncan et al.[13]	DPF (newborn heads)=5.4±0.5 (690 nm), 4.7±0.6 (832 nm), source-detector separation of 4.5 cm
Benaron et al.[14]	DPF (infant heads)=3.7±0.3 (754 nm, 816 nm), (source-detector separation of 1 mm)
Duncan et al.[15]	DPF (adult muscle)=6.5±1.1 (690 nm), 5.9±1.0 (832 nm), source-detector separation of 4.5 cm
Essenpreis et al.[9]	DPF (adult muscle)=5.7±0.6 (800 nm), source-detector separation of 4 cm
Matcher et al.[16]	DPF (adult muscle)=4.9±0.5 (820 nm), 2.8±0.3 (975 nm), source detector separation of 3.5 cm

DPF=mean path length/optode separation

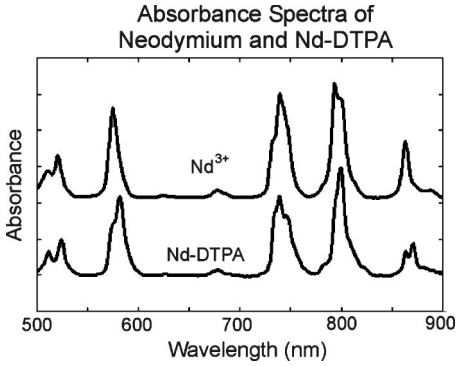

Fig. 1 Absorbance spectra of neodymium (Nd). Binding Nd to DTPA does not substantially change its absorbance spectrum.

In this paper, we introduce a novel method of measuring relative path length values using chromophores that exhibit multiple absorptions in the visible/near-IR spectrum. Since absorption intensity is proportional to path length, the relative absorption intensities for a single chromophore *in vivo* can be interpreted to yield relative path length values at the absorption wavelengths. To assess path length most accurately, a chromophore with as many distinct (and intense) absorptions as possible within the wavelength range of interest is desirable. Neodymium (Nd) is a lanthanide metal in the same row of the periodic table as gadolinium and dysprosium, both of which have been used clinically as contrast agents in magnetic resonance imaging studies.[20,21] Nd has several absorptions in the visible and near-IR regions, making it attractive for the present purpose[22,23] (Fig. 1), and when bound to a chelating agent such as diethylene-triamine-pentaacetic acid (DTPA), it is nontoxic with only minimal alteration to its absorbance spectrum.

Nd-DTPA exhibits distinct, narrow absorptions at 512 and 524 nm [overlapping peaks with a full bandwidth at half maximum (FWHM) of 19 nm], 582 nm (FWHM=15 nm), 679 nm (11 nm), 740 nm (19 nm), 800 nm (12 nm), and 864 and 871 nm (overlapping with FWHM of 12 nm). To exploit these absorptions *in vivo*, visible/near-IR point spectroscopy was carried out for isolated, beating hearts for which Nd-DTPA had been added to the coronary perfusion medium (perfusate). In this experimental arrangement, Nd-DTPA is distributed throughout the vasculature and enters the interstitial space, but does not penetrate the intact cell membranes. The relative intensities of the absorptions as they appear in spectra measured *in vivo* differ from the relative intensities as they appear *in vitro*, and these differences in relative intensity can be interpreted to quantify the wavelength dependence of effective optical path length. Water also exhibits absorptions at 835 and 975 nm that may be exploited similarly. The following experiments were therefore designed to capitalize on the

absorptions of Nd and water to determine the wavelength dependence of optical path length in spectroscopy of isolated rat hearts.

2 Materials and Methods

2.1 *Experimental Protocol*

To avoid possible spectroscopic interference of hemoglobin (Hb) absorptions with those of Nd, hearts were perfused with phosphate-free Krebs-Henseleit buffer* (KHB). Separate solutions of KHB with and without neodymium were prepared. To maximize the Nd absorption intensity and hence optimize the spectroscopic SNR, preliminary experiments were executed to determine the maximum Nd concentration that the heart could tolerate. To that end, varying concentrations of a Nd stock solution† were added to low-sodium KHB solutions to bring the Nd concentration to between 5 and 30 mM (the sodium content of the KHB was reduced to compensate for sodium contributions from the Nd stock solution). The maximum acceptable Nd concentration was deemed to be 20 mM. When the Nd concentration exceeded this value, adjustments to the KHB solution could not maintain free sodium, calcium, and potassium ion concentrations at normal levels. Since Nd-DTPA binds Ca^{++}, $CaCl_2$ was also added to the perfusate to restore ion concentrations to normal levels.

Sprague-Dawley rats ($n=11$) weighing 300 to 400 g were anesthetized with pentobarbital (120 mg/kg, intraperitoneally). When the animal was unresponsive to the toe pinch test, the chest cavity was opened and the heart was removed. The heart was then attached to a Langendorff perfusion setup and perfused through the aorta with phosphate-free KHB. The perfusate was bubbled with 95% O_2/5% CO_2 to maintain pO_2 at 500 to 600 mm Hg and pH at 7.35 to 7.45. Perfusion with this buffer was maintained for a minimum of 10 min to enable the heart's functional parameters to reach equilibrium.

Spectra were acquired continuously (2 s acquisition time) throughout the experimental protocol (400 to 1100 nm, 0.5-nm spacing). Broadband visible/near-IR light from a fiber optic illuminator (Oriel Model 77501, Stratford, Connecticut) was transmitted to the heart through one arm of a bifurcated fiber optic bundle. The common illumination/collection probe tip was placed in gentle contact with the heart, where scattered light was gathered and transmitted through the other arm of the fiber bundle to a visible/near-IR spectrometer (Control Developments, Inc.). The emitting and collecting fiber optic filaments [200-μm diameter, numerical aperture (NA)=0.22] were arranged in two concentric rings at the probe tip (collecting filaments formed the inner ring and emitting filaments formed the outer ring; the diameters were 2 and 6 mm, respectively). Sets of 10 spectra were averaged to increase SNR, yielding one spectrum every 20 s.

Following 5 min of baseline perfusion with regular KHB, hearts were perfused with the KHB to which Nd had been added (Nd-KHB) for 20 min. Perfusion was then switched back to Nd-free KHB and spectra were acquired for an additional 10 min. To verify that this Nd concentration (20 mM) did not adversely affect cardiac function, functional data were recorded every minute throughout the protocol.

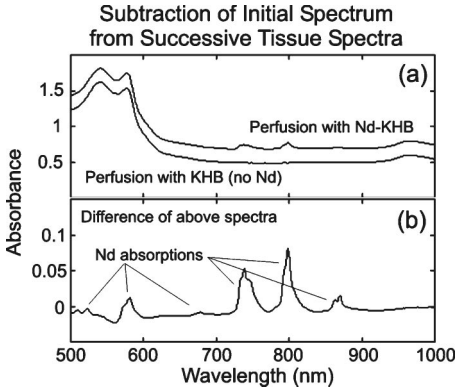

Fig. 2 (a) Sample tissue spectra acquired during perfusion with Nd-free KHB and KHB with a 20-mM Nd concentration. (b) Differences in the spectra are almost entirely due to Nd contributions.

2.2 *Spectral Analysis*

The only Nd absorptions clearly visible in the absorbance spectra were those at 740, 800, and 870 nm [Fig. 2(a)]. The mean of tissue spectra acquired during baseline perfusion (prior to addition of Nd) was calculated and subtracted from each spectrum acquired during the trial; these difference spectra clearly revealed the other Nd absorptions [Fig. 2(b)]. Assuming that Mb oxygenation, cytochrome redox state, and water content are unaffected by the presence of Nd, the contributions of these chromophores to the absorption profile should be eliminated in the difference spectra. This expectation has been validated previously for low (5 mM) concentrations of neodymium,[25] and was generally true for the trials within this study. However, 4 of the 11 trials did exhibit intensity changes in cytochrome and myoglobin absorptions when 20-mM Nd-DTPA was present in the perfusate. Since these spectral changes prevented clear visualization of the Nd absorptions, these trials were excluded from our analysis.

The difference spectra following addition of Nd were dominated by the Nd absorptions [Fig. 2(b)]. To compensate for small, residual non-Nd contributions to the spectra, a baseline was calculated for each difference spectrum, using a linear interpolation of the absorbance values on either side of each Nd absorption. These baselines were subtracted from the corresponding difference spectra.

The ratio of the *in vivo* absorption intensity to the *in vitro* absorption intensity (i.e., molar absorptivity) is the product of the concentration (which is constant for all wavelengths) and the path length:

$$(A_{in\ vivo}/\epsilon_{in\ vitro})_\lambda = CL_\lambda$$

This intensity ratio was determined for each Nd absorption and then normalized to the corresponding value for the 800-nm band, to provide the relative path length at each wavelength (since the concentration was uniform).

*KHB is a Hb-free solution, containing (in mM): NaCl (118), $NaHCO_3$ (25), KCl (4.7), $CaCl_2$ (1.75), $MgSO_4$ (1.2), EDTA-2Na (0.5), and glucose (11). It has been shown[24] to effectively transport oxygen (dissolved in the solution).

†Stock solutions of the Nd chelate (100 mM) were prepared by mixing equimolar amounts of $NdCl_3$ and DTPA (free acid). The acidic solution was titrated by NaOH to bring the pH to 7.4, which corresponded to mono-Na salt of DTPA (Nd-DTPA-Na·3NaCl).

Table 3 Cardiac functional parameters.

Heart	Baseline ($n=11$)	15 min. Nd-KHB Perfusion ($n=11$)
Heart rate [beats per minute (bpm)]	225±17	224±18 (NS)
Systolic pressure (mm Hg)	103±10	101±17 (NS)
Diastolic pressure (mm Hg)	7±2	7±3 (NS)
Pressure-rate product	21,600±3000	21,200±4500 (NS)
Perfusion pressure	66±2	74±12 ($p<0.05$)
Perf press/coronary flow	4.6±0.4	5.2±1.0 ($p<0.05$)

3 Results

3.1 *Neodymium Absorptions*

The effects of Nd-KHB perfusion on cardiac function are summarized in Table 3. While there was a small increase in perfusion pressure and coronary resistance upon perfusion with Nd-KHB, there was no significant effect on heart rate or systolic or diastolic pressure. These data confirm that addition of 20-mM Nd-DTPA to the perfusate did not adversely affect cardiac function.

The difference spectrum plotted in Fig. 2(b) clearly demonstrates that the visible-wavelength Nd absorptions (520, 580 nm) are much less intense relative to the near-IR bands *in vivo* than they are *in vitro* (Fig. 1). The deoxy-Hb absorptions show a parallel trend, with the intensity of the 555-nm band relative to that of the 760-nm band reduced *in vivo* (unpublished observations). Both chromophores therefore lead to the conclusion that near-IR light travels a greater distance through the tissue than visible light.

As illustrated in Fig. 3, optical path length reaches a maximum near 800 nm, falling rapidly with increasing wavelength and more gradually with decreasing wavelength. The results are also much more precise for the strong near-IR bands than for the weaker visible bands, due both to the high absorption intensity and to the fact that no other absorptions interfere with them. The path lengths at 679, 740, and 870 nm are 90±9%, 94±1%, and 84±1% of the path length at 800 nm, respectively. In contrast, the path lengths at 520 and 580 nm were 41±13% and 49±21% of the path length at 800 nm. These results are not consistent with published DPF data, which suggest that path length decreases with increasing wavelength in the range between 690 and 860 nm, but they are consistent with the prevalent notion, originally forwarded by Jöbsis in his seminal 1977 paper, that the near-IR offers a ''therapeutic window'' due to the deep penetration of near-IR as compared to visible light.[3]

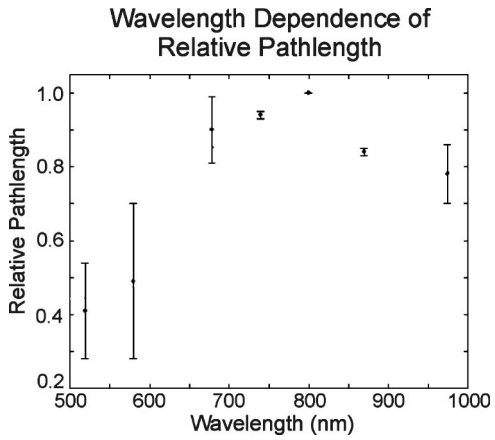

Fig. 3 Path lengths at 520, 580, 679, 740, and 870 nm (neodymium absorptions) and 975 nm (water absorption) relative to that at 800 nm (neodymium absorption), as determined by normalized relative neodymium and water absorption intensities in isolated rat hearts ($n=7$).

These results, and the observed difference spectra, explain why only the three near-IR absorptions appear prominently in *in vivo* spectra. The 679-nm absorption is too weak to be visible without preprocessing, and the 520- and 580-nm absorptions are attenuated by relatively short path length and suffer from interference by the myoglobin and cytochrome absorptions.

3.2 *Water Absorption*

The most intense water absorption in the 500- to 1100-nm range is at 975 nm. A much weaker absorption is present at 835 nm (the water absorption at 730 nm proved too weak to observe in these spectra), and the only other endogenous chromophore absorbing significantly in the 800–1000 nm region is myoglobin. Since the perfusate was well-oxygenated, the deoxy-Mb concentration was negligible. While the oxy-Mb band centered at 920 nm does overlap with the water bands, this absorption is extremely broad relative to those of water, and therefore its contribution can be effectively suppressed by taking the second derivative of the tissue spectra.[16]

The second derivative of a representative cardiac tissue spectrum (acquired during normal perfusion with Nd-free KHB) and of the water absorptivity spectrum are displayed in Fig. 4. Both spectral features attributable to water (near 835 and 975 nm) are clearly visible, although the features observed in tissue spectra are shifted by a few nanometers relative to the corresponding bands in the absorptivity spectrum (this may be due to interactions of water with various biological microenvironments, a factor that also broadens the 975-nm band). When the spectra are scaled to a common intensity for the feature at 835 nm, the 975-nm absorption for

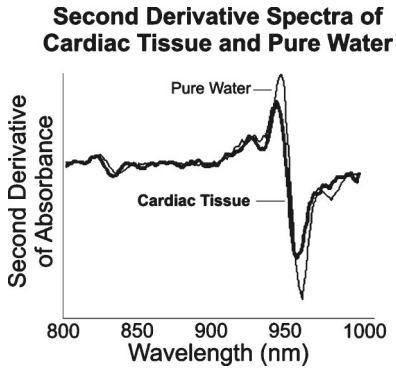

Fig. 4 Intensity of the second derivative of the 975-nm water absorption relative to that of the 835-nm absorption is lower in tissue than *in vitro*.

tissue water is clearly weaker than the corresponding band for pure water. This suggests that the optical path length is shorter at 975 than at 835 nm.

To quantify this relationship, the ratio I_{975}/I_{835} was evaluated for (second derivative) spectra representative of each heart, as well as for the water absorptivity spectrum. The relative path length at 975 versus 835 nm was then calculated by dividing the *in vivo* intensity ratio (heart) by the *in vitro* ratio (water absorptivity), yielding the conclusion that the path length at 975 nm is 83±9% of that at 835 nm. The variance may be due to subtle variability in probe placement against the cardiac tissue (affecting the path traveled by the photons) or genuine intersubject variability in tissue structure. To assimilate these results with the Nd analysis, the path length at 835 nm was estimated by interpolation of the Nd data to be 94% of that at 800 nm. This further implies that the path length at 975 nm is 78±8% of the path length at 800 nm. This relative path length value at 975 nm is included in the wavelength-dependence plot of Fig. 3.

The 835-nm absorption of water has been suggested previously to be useful as a probe of absolute path length in near-IR spectra of tissue.[16] By taking the second derivative, the contribution of the very broad HbO_2/MbO_2 absorption is essentially eliminated, leaving the water absorption as the only feature absorbing in the range 800 to 880 nm. If the concentration of water is known for the tissue of interest (e.g., the water content of brain tissue is ~90%), then the effective optical path length can be determined by fitting the observed (second differential) water absorption $A(\lambda)$ with the second derivative of the absorptivity spectrum for pure water $\epsilon(\lambda)$:

$$A(\lambda) = \epsilon(\lambda) cL.$$

The fitting coefficient is the product of concentration and path length cL, and dividing by the molar water concentration (e.g., 55.5 mol/L for pure water×90% water content for brain tissue yields a water content of 50 mmol/L) then yields the effective optical path length L.

4 Discussion

This method is unique in that it can provide relative optical path length data without extra equipment beyond that needed for the intended spectroscopic studies (e.g., no ultrashort-pulse-width lasers). Moreover, it can be performed for any experimental geometry; indeed, it should be repeated for each change in experimental geometry, since the wavelength dependence of optical path length will certainly change accordingly. Finally, the method outlined here can be refined by including additional exogenous chromophores with distinct absorptions to provide path length data for additional wavelengths within the spectral region of interest. Obvious candidates include other transition metals such as dysprosium or europium, each of which contributes a unique set of visible/near-IR absorptions.

The neodymium absorption intensities measured *in vivo* indicate no significant difference between path lengths at 520 and 580 nm. This conclusion is consistent with the fact that relative oxy-Mb absorption intensities at 540 and 580 nm in tissue spectra are comparable to those observed *in vitro*. The path length therefore varies little with wavelength between 500 and 600 nm. However, given the Nd data between 500 and 800 nm, a steep rise in path length must occur between 600 and 700 nm (Fig. 3).

It has been suggested that the absorptions of tissue chromophores shorten the optical path length, since there is an increased likelihood that photons will be absorbed in transit from the emitter to the detector.[26] The question that then arises is whether the absorptions of neodymium affect the optical path length, i.e., does the probe affect the quantity of interest? To assess this possibility, we have searched for literature examples wherein the optical path length was measured directly (using either phase- or time-resolved spectroscopy) at a single wavelength but varying the concentration of species absorbing at that wavelength. One clear example appears in a piglet cerebral study[27] wherein the path length was measured at 754 nm while the sagittal sinus hemoglobin saturation was varied from 4 to 98%. These variations in O_2 saturation would cause changes of ~0.1 absorbance units (or greater) at 754 nm due to variations in the intensity of the deoxyhemoglobin absorption centered at 758 nm (see, e.g., Ref. 28), yet the effective path length deviated by only −0.62 cm (during hypoxia) to 0.93 cm (during hyperoxia) from the value of 13.6 cm during normoxia. While these findings confirm that the path length does decrease with increasing absorbance, the measured change was less than 12% coincident with an absorption band spanning an absorbance range greater than 0.1 absorbance units. Since the absorptions of neodymium in this paper range in intensity from ~0.03 to 0.08 absorbance units (see Fig. 2), we conclude that their influence on path length should be less than 10%. Furthermore, the effect would be to fractionally shorten the effective path length at all neodymium absorption wavelengths, so that the error in relative path lengths determined from them would be substantially less than 10%.

While the approach outlined here provides a measure of the wavelength dependence of optical path length in tissue, water absorptions can be further exploited to provide an absolute measure of the optical path length, as described previously.[16] Since the water concentration in cardiac tissue is known, the 975-nm absorption of water can be used to determine the path length. Reconfiguring the Beer-Lambert law, the path length L can be expressed as a function of the absorbance A, the molar absorptivity ϵ, the concentration C: $L = A/(\epsilon C)$. The (baseline-corrected) absorbance and absorp-

tivity values are known. Since water constitutes 77% of the weight of KHB-perfused hearts,[29] the concentration is approximately 43 M. This provides a path length of 3.8 ± 0.6 mm. Expressed as a multiple of the radial spacing between the emitting and collecting fibers (2 mm), the DPF value comes to 1.86 ± 0.31. This result, combined with the relative path length values already listed, yields absolute path lengths at 520, 580, 679, 740, 800, 870, and 975 nm of 2.0, 2.4, 4.4, 4.6, 4.9, 4.1, and 3.8 mm, respectively.

It is surprising at first glance that the effective optical path length has a maximum at 800 nm, decreasing from this maximum value to both shorter and longer wavelengths. This is apparently at variance with the studies cited in Table 2; for those investigations that include determination of path length (or, equivalently, the DPF) at two or more wavelengths, the path length at the longer wavelength has generally been found to be shorter than that observed for shorter wavelength. The qualitative discrepancy may originate from any of a number of factors. First, the majority of published DPF determinations have been either for cerebral studies or for skeletal muscle. Although it is generally agreed that the brain is sampled by optodes placed sufficiently far apart on the scalp, the tissue volume probed by this arrangement includes the skin, scalp tissue, skull, and meninges in addition to the brain tissue itself. It would not be surprising if the mean path traversed by photons in this arrangement were quite different from that for the same probe arrangement on cardiac tissue, and if the wavelength dependence of the effective path length differed from that for cardiac tissue. For skeletal muscle studies, the photons that reach the detecting fiber travel through layers of skin and fat before entering and after exiting the muscle tissue itself.

Additional factors that distinguish the measurements reported here from the majority of previous studies are the arrangement of the transmitting and receiving fibers in concentric rings, and the relatively short interoptode spacing (since emission and receiving fibers are arranged in concentric rings of diameter 2 and 6 mm, respectively, the physical distance between emitting and receiving fibers spans the range 2 to 4 mm). It is not clear what role these considerations might play in governing the wavelength dependence of optical path length, and for that reason it would be of interest to carry out separate measurements for neodymium-perfused tissue with optode spacing more closely similar to that used for previous path length measurements. While such experiments are impracticable for rat hearts, they may be considered for larger hearts, e.g., for pigs. Such experiments are now planned and will be reported separately.

This paper demonstrates the utility of neodymium chelates for the determination of optical properties in tissue. We have also previously demonstrated[25] that neodymium chelates can be used effectively as contrast agents to identify irreversibly damaged tissue (i.e., tissue with significant membrane damage). While lanthanides have been widely used as contrast agents in magnetic resonance studies, these results indicate a rich potential for the use of lanthanides such as neodymium in optical tissue diagnostics.

5 Conclusion

The combined information available from an exogenous agent (Nd) and an endogenous chromophore (water) was interpreted to provide both a measure of relative path length in tissue as a function of wavelength and an absolute measure of path length. While these results are interesting in their own right, they also have practical application in the analysis of *in vivo* spectra. Knowledge of the relative and absolute path lengths enables more exact quantitative spectroscopic determination of chromophore concentrations. While the results presented here apply strictly for this experimental setup only (an optical probe with emission and collection fibers in concentric rings with a radial spacing of 2 mm), the method opens the door to determining the wavelength dependence of path length for any experimental arrangement. Indeed, it would be of interest to assess the effect of geometry and interoptode spacing on the wavelength dependence, and experiments are planned to that end.

Acknowledgments

The authors would like to recognize Bozena Kuzio for her assistance with the experimental protocol. This research was funded by a grant from the Canadian Institutes for Health Research.

References

1. I. Giannini, M. Ferrari, A. Carpi, and P. Fasella, ''Rat brain monitoring by near-infrared spectroscopy: an assessment of possible clinical significance,'' *Physiol. Chem. Phys.* **14**, 295–305 (1982).
2. W. J. Parsons, J. C. Rembert, R. P. Bauman, J. C. Greenfield, Jr., and C. A. Piantadosi, ''Dynamic mechanisms of cardiac oxygenation during brief ischemia and reperfusion,'' *Am. J. Physiol.* **259**, H1477–H1485 (1990).
3. F. F. Jöbsis, ''Noninvasive, infrared monitoring of cerebral and myocardial oxygen sufficiency and circulatory parameters,'' *Science* **198**, 1264–1267 (1977).
4. J. M. Schmitt, H. Yang, and J. N. Qu, ''Interpretation and processing of NIR spectra of turbid biological tissue,'' *Proc. SPIE* **3257**, 134–145 (1998).
5. G. Kumar and J. M. Schmitt, ''Optimal probe geometry for near-infrared spectroscopy of biological tissue,'' *Appl. Opt.* **36**, 2286–2293 (1997).
6. A. D. Hunter, J. A. Crowe, and J. G. Walker, ''Measurement of in vivo hemoglobin concentration using diffuse reflectance,'' *Proc. SPIE* **3566**, 88–96 (1998).
7. D. A. Benaron and D. K. Stevenson, ''Optical time-of-flight and absorbance imaging of biologic media,'' *Science* **259**, 1463–1466 (1993).
8. D. T. Delpy and M. Cope, ''Quantification in tissue near-infrared spectroscopy,'' *Philos. Trans. R. Soc. London, Ser. B* **352**, 649–659 (1997).
9. M. Essenpreis, C. E. Elwell, M. Cope, P. van der Zee, S. Arridge, and D. T. Delpy, ''Spectral dependence of temporal point spread functions in human tissues,'' *Appl. Opt.* **32**, 418–425 (1993).
10. L. M. Klassen, B. J. MacIntosh, and R. S. Menon, ''Influence of hypoxia on wavelength dependence of differential pathlength and near-infrared quantification,'' *Phys. Med. Biol.* **47**, 1573–1589 (2002).
11. J. Pringle, C. Roberts, M. Kohl, and P. Lekeux, ''Near infrared spectroscopy in large animals: optical pathlength and influence of hair covering and epidermal pigmentation,'' *Vet. J.* **158**, 48–52 (1999).
12. M. Kohl, C. Nolte, H. R. Heekeren, S. Horst, U. Scholz, H. Obrig, and A. Villringer, ''Determination of the wavelength dependence of the differential pathlength factor from near-infrared pulse signals,'' *Phys. Med. Biol.* **43**, 1771–1782 (1998).
13. A. Duncan, J. H. Meek, M. Clemence, C. E. Elwell, P. Fallon, L. Tyszczuk, M. Cope, and D. T. Delpy, ''Measurement of cranial optical path length as a function of age using phase resolved near infrared spectroscopy,'' *Pediatr. Res.* **39**, 889–894 (1996).
14. D. A. Benaron, C. D. Kurth, J. M. Steven, M. Delivoria-Papadopoulos, and B. Chance, ''Transcranial optical path length in

infants by near-infrared phase-shift spectroscopy,'' *J. Clin. Monit* **11**, 109–117 (1995).
15. A. Duncan, J. H. Meek, M. Clemence, C. E. Elwell, L. Tyszczuk, M. Cope, and D. T. Delpy, ''Optical pathlength measurements on adult head, calf and forearm and the head of the newborn infant using phase resolved optical spectroscopy,'' *Phys. Med. Biol.* **40**, 295–304 (1995).
16. S. J. Matcher, M. Cope, and D. T. Delpy, ''Use of the water absorption spectrum to quantify tissue chromophore concentration changes in near-infrared spectroscopy,'' *Phys. Med. Biol.* **38**, 177–196 (1993).
17. B. de Groot, C. J. Zuurbier, and J. H. van Beek, ''Dynamics of tissue oxygenation in isolated rabbit heart as measured with near-infrared spectroscopy,'' *Am. J. Physiol.* **276**, H1616–H1624 (1999).
18. D. A. Benaron and D. K. Stevenson, ''Resolution of near infrared time-of-flight brain oxygenation imaging,'' in *Oxygen Transport to Tissue XV*, P. E. A. Vaupel, Ed., pp. 609–617, Plenum Press, New York (1994).
19. D. T. Delpy, M. Cope, P. van der Zee, S. Arridge, S. Wray, and J. Wyatt, ''Estimation of optical pathlength through tissue from direct time of flight measurement,'' *Phys. Med. Biol.* **33**, 1433–1442 (1988).
20. N. Al-Saadi, E. Nagel, M. Gross, A. Bornstedt, B. Schnackenburg, C. Klein, W. Klimek, H. Oswald, and E. Fleck, ''Noninvasive detection of myocardial ischemia from perfusion reserve based on cardiovascular magnetic resonance,'' *Circulation* **101**, 1379–1383 (2000).
21. J. Ornac, M. C. Schmidt, P. Theissen, and U. Sechtem, ''Assessment of myocardial perfusion by magnetic resonance imaging,'' *Herz* **22**, 16–28 (1997).
22. L. R. P. Kassab, L. C. Courrol, N. U. Wetter, S. H. Tatumi, and C. M. S. P. Mendes, ''Glasses of heavy metal and gallium oxides doped with neodymium,'' *Radiat. Eff. Defects Solids* **156**, 371–375 (2001).
23. A. M. Tkachuk, S. E. Ivanova, L. I. Isaenko, A. P. Yelisseyev, S. Payne, R. Solarz, R. Page, and M. Nostrand, ''Spectroscopic study of neodymium-doped potassium-lead double chloride Nd^{+3}:KPb_2Cl_5 crystals,'' *Opt. Spectrosc.* **92**, 83–94 (2002).
24. V. V. Kupriyanov, B. Xiang, K. W. Butler, M. St Jean, and R. Deslauriers, ''Energy metabolism, intracellular Na+ and contractile function in isolated pig and rat hearts during cardioplegic ischemia and reperfusion: ^{23}Na- and ^{31}P-NMR studies,'' *Basic Res. Cardiol.* **90**, 220–233 (1995).
25. S. P. Nighswander-Rempel, R. A. Shaw, B. Kuzio, and V. V. Kupriyanov, ''Detection of myocardial cell damage in isolated rat hearts with near-infrared spectroscopy,'' *J. Biomed. Opt.* **9**, 779–787 (2004).
26. J. E. Brazy, D. V. Lewis, M. H. Mitnick, and F. F. Jöbsis-Vander Vliet, ''Monitoring of cerebral oxygenation in the intensive care nursery,'' *Adv. Exp. Med. Biol.* **191**, 843–848 (1985).
27. D. A. Benaron, C. D. Kurth, J. Steven, L. C. Wagerle, B. Chance, and M. Delivoria-Papadopoulos, ''Non-invasive estimation of cerebral oxygenation and oxygen consumption using phase-shift spectrophotometry,'' *Proc. IEEE* **12**, 2004–2006 (1990).
28. T. Kusaka, K. Isobe, K. Nagano, K. Okubo, S. Yasuda, M. Kondo, S. Itoh, K. Hirao, and S. Onishi, ''Quantification of cerebral oxygenation by full-spectrum near-infrared spectroscopy using a two-point method,'' *Comp. Biochem. Physiol., Part A: Mol. Integr. Physiol.* **132**, 121–132 (2002).
29. P. I. Polimeni, ''Measurements of myocardial electrolyte distribution,'' in *Techniques in the Life Sciences, P3/II: Cardiovascular Physiology, P317*, pp. 1–34, Elsevier Scientific, County Clare, Ireland (1984).